Controller Design of Stand-Alone Photovoltaic System with Charge-Discharge Controller for Remote Island Power Supply

Hong-Sung Kim Gwon-Jong Yu Jinsoo Song Young-Seok Jeong
Ki-Hwan Kang Byoung-Ku Lee *Gyu-Ha Choe

Korea Institute of Energy Research
71-2, Jang-Dong, Yusong-Ku,
Taejon, 305-343 Korea

*** Dept. of E.E, Kon-Kuk Univ.**
93-1, Mojin-Dong, Kwangjin-Gu,
Seoul, Korea

Abstract - This paper deals with stand-alone Photovoltaic system(SPVS) with charge and discharge controller. Main power source of SPVS are generally solar cell and battery. Therefore SPVS can be classified into variable types in accordance with connection method between battery and solar cell array. Mainly used one of them is direct connection type which has advantages such as simple structure and simple controller. However most big drawback of this system is energy loss by voltage disharmony between solar cell array and battery. Therefore SPVS with charge and discharge controller which can operate solar cell array at maximum power point is designed and experimented with a laboratory prototype.

1. Introduction

Stand-alone photovoltaic system(SPVS) is installed in about 4 islands of west-sea zone where utility power can not be supplied and is operated as main energy source. SPVS can be considered as generation method competitive with conventional one with considering that 270 of 518 man living islands in korea are under limited supplying by diesel generator or can't be supplied at all[1].

Main power source of SPVS is solar cell and battery. Therefore SPVS can be classified into variable types in accordance with connection type between battery and solar cell array. Mainly used one of them is direct connection type which has advantages such as simple structure and controller. However most big drawback of this system is energy loss by voltage disharmony between solar cell array and battery which reach to 15-50[%] according to battery open voltage.

Therefore SPVS with charge and discharge controller which can operate solar cell array at maximum power point and can reduce powerloss due to voltage disharmony is designed and verified by experiment in this paper.

2. SPVS Configuration

Fig. 1 describes the most simple SPVS in which battery and solar cell array are connected directly. This system has advantages such as simple structure and controller as above mentioned. However because of voltage disharmony due to relations between battery I-V characteristics and solar cell one like as fig. 2, solar cell can't operate at maximum power power point and energy loss occurs. This energy loss rate reach to 15[%] - 50[%] according to relations between battery open voltage and solar cell maximum power point voltage, minimum energy loss is to be given when the battery open voltage is 90[%]-95[%] of maximum power point voltage[2][3].

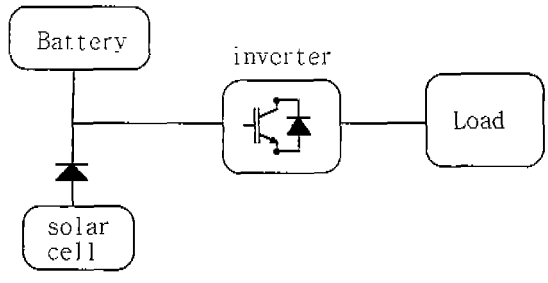

Fig. 1 Schematic diagram of parallel operation type stand-alone photovoltaic system

As fig.3, MPPT(maximum power point tracker) can be a remedy for decreasing power loss caused by voltage disharmony. This method can make solar cell to operate in maximum power point but there occurs voltage variation of inverter DC link. And also additional equipment is required for the protection of battery.

Therefore SPVS with charge and discharge controller in fig. 4 can be considered as a remedy for such defects. Because charge and discharge controller can control bidirectional power flow, it is possible to control DC voltage. This means that problem of power loss due to voltage disharmony can be solved.

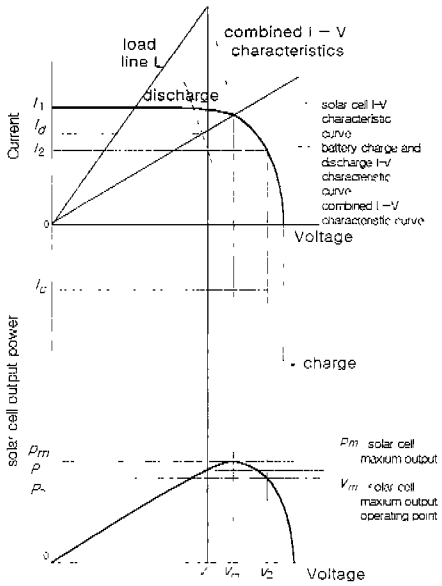

Fig. 2 Influence of battery on operating voltage of solar cell

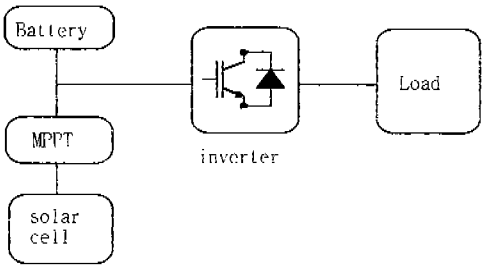

Fig. 3 Schematic diagram of system with MPPT

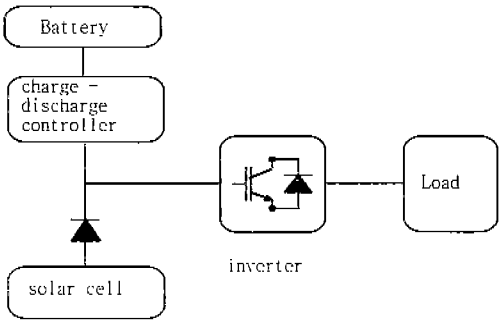

Fig. 4 Schematic diagram of stand-alone photovoltaic system with charge and discharge controller

Fig. 5 shows power circuit of SPVS with charge and discharge controller used in this paper.

3. System model

In the system modelling, inductance, capacitor, switch and transformer are assumed as ideal elements. Differential equations of charge and discharge controller are expressed as followings.

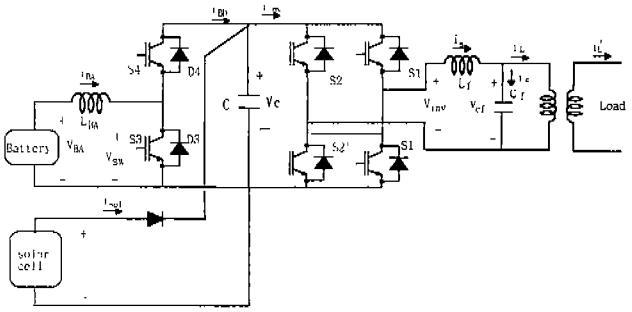

Fig. 5 stand-alone photovoltaic system with charge and discharge controller

$$\frac{di_{BA}}{dt} = (V_{BA} - V_{SW})/L_{BA} \quad (1)$$

$$\frac{dV_C}{dt} = (i_{BD} + i_{sol} - i_{inv})/C \quad (2)$$

The expression of switch voltage Vsw according to operation mode and the input current i_{BD} to DC link capacitor is expressed like following equations.

- Operation as discharge controller (S3, D4 used)

S=1 : S3 on S=0 : S3 off

$V_{SW} = (1-s)\,V_C \qquad i_{BD} = (1-s)i_{BA}$

- Operation as charge controller (S4, D3 used)

S=1 : S4 on S=0 : S4 off

$V_{SW} = sV_C \qquad i_{BD} = si_{BA}$

And followings are expression of inverter circuit.

$$\frac{di_s}{dt} = (V_{inv} - V_{cf})/L_f \quad (3)$$

$$\frac{dV_{Cf}}{dt} = (i_s - i_l)/C_f \quad (4)$$

where $V_{inv} = S_{inv}V_C$

S_{inv} : inverter switching function

The DC link current i_{inv} is described as follows.

$$i_{inv} = S_{inv}i_s \quad (5)$$

And then following equation describes approximate Solar cell output current.

$$i_{sol} = i_{sc}(1 - \exp(K(\frac{V_c}{V_{oc}} - 1))) \quad (6)$$

where K : curve constant
Voc : solar cell open voltage
isc : solar cell short current

4. Controller design

System controller is composed of DC/AC inverter, and charge-discharge controller. The charge - discharge controller has a function of DC voltage regulation by power balancing contol between solar cell and AC load. And Power balancing control is possible by bidirectional current control. DC/AC inverter has a funtion to control a AC filter capacitor voltage to be CVCF(constant frequency and constant voltage).

(1) DC/AC inverter

The inverter controller consists of current controller - inner loop and voltage controller - outer loop.
As a current controller, used is Predictive controller as followings.

$$V_{inv}^{*}(k)=\frac{L_f}{T_s}(\ i_s^{*}(k+1)-i_s(k))+V_{cf}(k) \quad (7)$$

where Ts : sampling time

Using simple backward difference approximation[4], eq.(3) can be described as following difference equation.

$$V_{inv}(k)=\frac{L_f}{T_s}(\ i_s(k+1)-i_s(k))+V_{cf}(k) \quad (8)$$

Provided that inverter modulator and process are ideal, inverter output voltage reference - eq.(7) is same with real inverter output voltage. Therefore substituting eq.(7) into $V_{inv}(k)$ of eq(8), following equation is obtained. From this equation we can know that predictive controller has unity gain.

$$i_s(k+1)=\ i_s(k+1)^{*} \quad (9)$$

And then current reference of eq.(9) is obtained by PI controller output added to load current (i_L) which appers as disturbance in control loop.

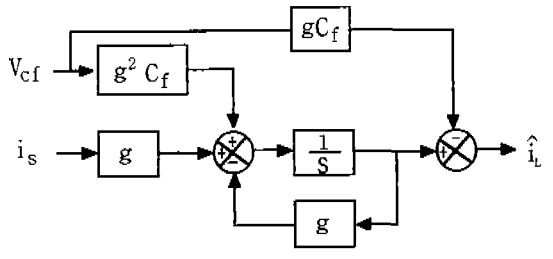

Fig. 6 load current observer

And load current is estimated by observer like as fig.6. The observed load current is expressed as eq.10 in continuous domain and estimation speed is dependent of observer gain g.

$$\widehat{i_L}=\frac{g}{S+g}(i_s-C_fSV_{cf}) \quad (10)$$

where g : observer gain

In case using digital controller, observer gain g is determinded to be below 1/6 of controller sampling frequency[4]. Therefore overall control block diagram is as follows.

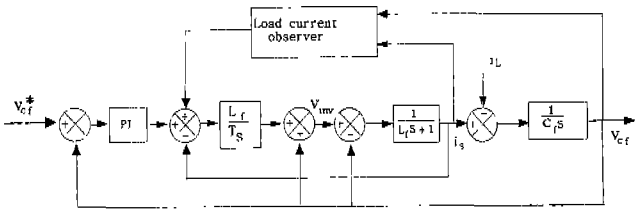

PI = Kp + Ki/s

Fig. 7 block diagram of inverter controller

Assuming that sampling time is short enough to be ignored and observer has nearly ideal characteristics, as current controller has unity gain, the system transfer function is expressed in continuous domain as the following equation.

$$\frac{V_{cf}}{V_{cf}^{*}}=\frac{\frac{K_p}{C_f}s+\frac{K_i}{C_f}}{s^2+\frac{K_p}{C_f}s+\frac{K_i}{C_f}} \quad (11)$$

Therefore gain of PI controller can be determined by proper pole placement as follows[5].

$$K_i=\ \omega_n{}^2 C_f$$
$$K_p=2\zeta\omega_n C_f$$

where ω_n : natural angular frequency
ζ : damping ratio

Unipolar switching method[6] of fig.8 is used conceptually as modulator. In case inverter output voltage reference is larger than zero, on time of Inverter switch S1, S2 is calculated as table1.

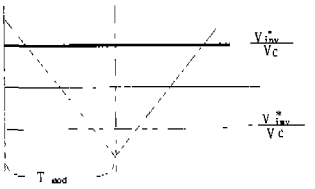

Fig. 8 Schematic diagram for modulator design

(2) charge-discharge controller

The charge-discharge controller has a function of dc voltage regulation by bidirectional power control. Control loop of this system is composed of two loop

similar with inverter as fig. 9. A current controller is designed as follows.

$$V_{sw}^{*}(k) = \frac{L_{BA}}{T_s}\left(i_{BA}^{*}(k+1) - i_{BA}(k)\right) + V_{BA}(k) \quad (12)$$

Table 1. Inverter modulator design

	S_1 on time	S_2 on time
$V_{inv}^{*} > 0$	$0.5T_{\mathrm{mod}} + 0.5\frac{V_{inv}^{*}}{V_C} Tmoa$	$0.5T_{\mathrm{mod}} - 0.5\frac{V_{inv}^{*}}{V_C} Tmoa$
$V_{inv}^{*} < 0$	$0.5T_{\mathrm{mod}} - 0.5\frac{V_{inv}^{*}}{V_C} Tmoa$	$0.5T_{\mathrm{mod}} + 0.5\frac{V_{inv}^{*}}{V_C} Tmoa$

The current reference is obtained as (eq).14 using PI controller and instantaneous power balance equation eq. (13) .

$$V_{BA}i_{BA} = V_C i_{BD} = V_{inv}i_s - V_C i_{sol} + system\ loss \quad (13)$$

$$i_{BA}^{*} = \left(V_C^{*} - V_C\right)\left(K_{pd} + \frac{K_{id}}{s}\right) + \frac{\left(V_{inv}^{*} i_s - V_C i_{sol}\right)}{V_{BA}} \quad (14)$$

By eq.(14), we can know that system loss of eq.(13) is compansated by PI controller. And modulator is designed as the following table.

Table 2. Modulator design according to current reference direction

	S3	S4	on time
$i_{BA}^{*} > 0$	use	no use	$T_{\mathrm{mod}} - \frac{V_{sw}^{*}}{V_C} T_{\mathrm{mod}}$
$i_{BA}^{*} < 0$	no use	use	$\frac{V_{sw}^{*}}{V_C} T_{\mathrm{mod}}$

Because charge-discharge controller operates as step-up chopper or step-down chopper according to current direction, switch on time is calculated differently in accordance with current direction. Consequently control block diagram of charge-discharge controller is like as fig. 9. The Gain of PI controller of fig.9 is determined under assumptions that modulator is ideal, current controller has unity gain. Using (eq).13, the charger-discharger output current i_{BD} is as eq.(15).

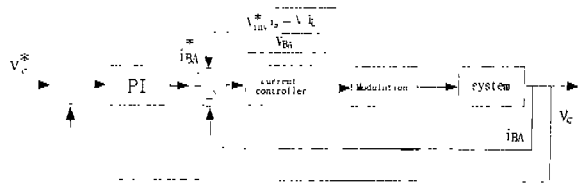

Fig. 9 block diagram of charge and discharge controller

$$i_{BD} = \frac{V_{BA}i_{BA}}{V_C} = V_{BA}i_{BA}P_g \quad (15)$$

where Pg = 1/Vc

In above equation, power gain Pg is can be linearized about nominal point using taylor series as follows.

$$P_g = \frac{1}{V_C^{*}} + \frac{1}{V_C^{*2}}\left(V_C - V_C^{*}\right) \quad (16)$$

where V_C^{*} : nominal operating point (DC voltage reference)

Because the second term of right one of eq.(16) is negligible, eq.(16) can be expressed approximately as follows:

$$i_{BD} = \frac{V_{BA}i_{BA}}{V_C^{*}} = K_{cg}i_{BA} \quad (17)$$

where $K_{cg} = \frac{V_{BA}}{V_C^{*}}$

The approximated control loop of charge-discharge controller is as fig. 10.

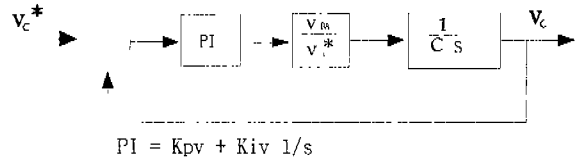

Fig.10. Approximated control loop

And the following equation describes transfer function of fig.10.

$$\frac{V_c}{V_c^{*}} = \frac{\frac{k_{cg}K_{pv}}{C}s + \frac{k_{cg}K_{iv}}{C}}{s^2 + \frac{k_{cg}K_{pv}}{C}s + \frac{k_{cg}K_{iv}}{C}} \quad (18)$$

Therefore controller gain can be determined by proper pole placement.

5. Experimental results

Experimental results which verify system operation was showed in this chapter. The Experimental condition is described in table 3. And TMS320C31 was used as controller.

Table 3. Experimental condition

Lf	1.2 [mH]
Cf	100 [μF]
Vcf	$\sqrt{2}.100.\sin(\omega t)$
DC Voltage	240[V]
C	8500 [μF]
LBA	2.7 [mH]
natural angular frequency of Inverter controller	2199 [rad/sec]
natural angular frequency of charge-discharge controller	18.9 [rad/sec]
Sampling time (Ts)	100[μsec]
Modulator sampling time (Tmod)	100[μsec]
Solar cell maximum output	2 [kW]

In laboratory, AC/DC converter constructed as fig.11 was used instead of battery.

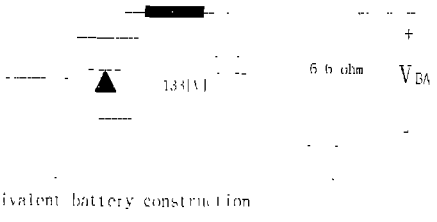

Fig. 11 Equivalent battery construction

(1) Inverter operating characteristics

Fig. 12 shows inverter operating characteristics when load condition is varying from no load to loading state. At the instant which load condition change, sinking of about 20[V] occurs at capacitor voltage (v_{cf}). And after about 15[msec], capacitor voltage reaches to steady state. And fig. 12(c) and (d) show FFT results before and after load variation. THD before and after load variation is simimilar and the magnitude of fundamental component is same.

Fig. 13 shows operating characteristics without using load current observer. THD results are very similar with the case using load observer. But reaching speed to steady state is lower, and we can see from FFT results that at loading state the magnitude of fundamental component decrease. At steady state voltage decrease is due to frequency characteristics of disturbance.

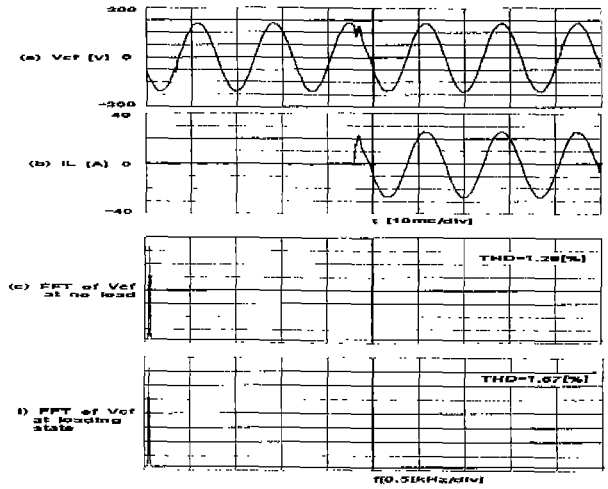

Fig. 12 Inverter operating characteristics with load current observer
(a) capacitor voltage (b) load current (c) voltage FFT at no load (d) voltage FFT at loading state

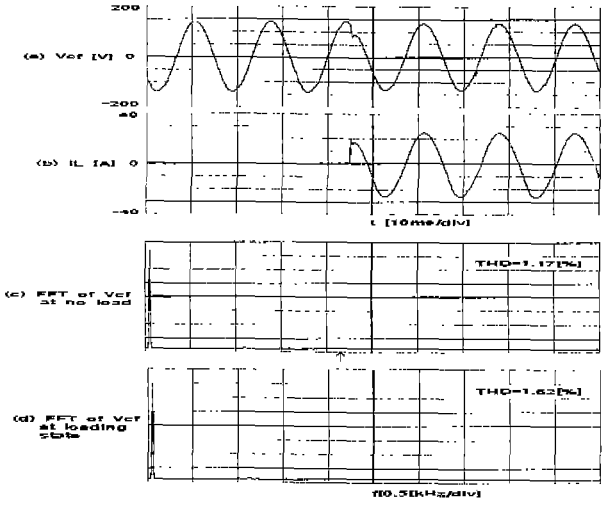

Fig. 13 Inverter operating characteristics without load current observer
(a) capacitor voltage (b) load current (c) voltage FFT at no load (d) voltage FFT at loading state

(2) Discharging mode - without solar cell output

In discharging mode which mainly occrus at night time or rainy day, system operating results are showed. Fig.14 is waveforms of system each part according to load condition. At no load state battery current(i_{BA}) is nearly zero. However at loading state, battery current which is composed of 120[Hz] component, DC component and high frequency component due to switching is transferred. In battery current, the generation of 120[Hz] component is due to feedforward control using power balance equation.

And DC voltage(Vc) is nearly constant at transient state. This means that current controller has a very rapid control characteristics. In order to show feedforward control effect, results without using feedforward control are described at fig.15. Compared to fig. 14, DC voltage has larger under shoot and over shoot at transient state. And battery current is composed of DC component and high frequency component. DC voltage variation at transient state is able to be improved by increasing control gains. However because increasing control gains is limited by noise problem and sampling frequency etc, feedforward control is needed. A drawback of feedforward control is current peak increase due to current reference generation based on instantaneous power control.

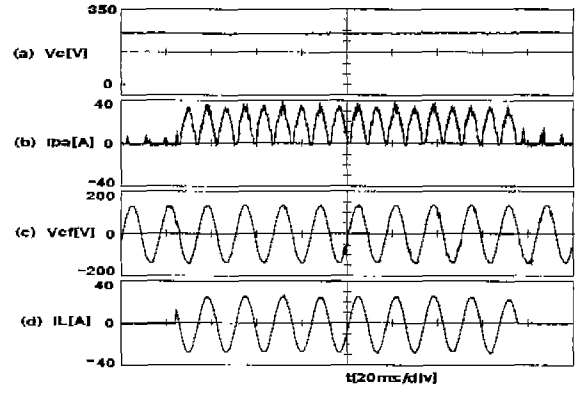

Fig. 14 Waveforms of system with feedforward control in discharging mode
(a) DC voltage (b) battery current
(c) capacitor voltage (d) load current

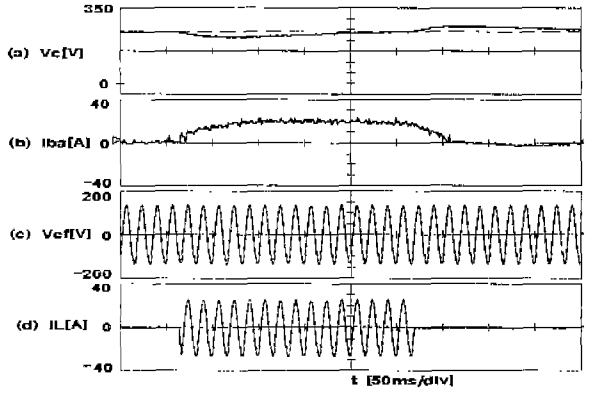

Fig. 15 system waveforms with feedforward control in discharging mode
(a) DC voltage (b) battery current
(c) capacitor voltage (d) load current

(2) Mode changing characteristics - with solar cell output

Fig. 16 shows system transient waveforms by load variation when solar cell out put is about 720[W]. At loading state, battery current swing sinusoidally with 120[Hz] between pluses and minuses. And the charge-discharge controller operates as charging mode at no load. Consequently tt is observered that bidirectional power control is smoothly made by operating mode change. And also at transient state DC voltage regulation is smooth.

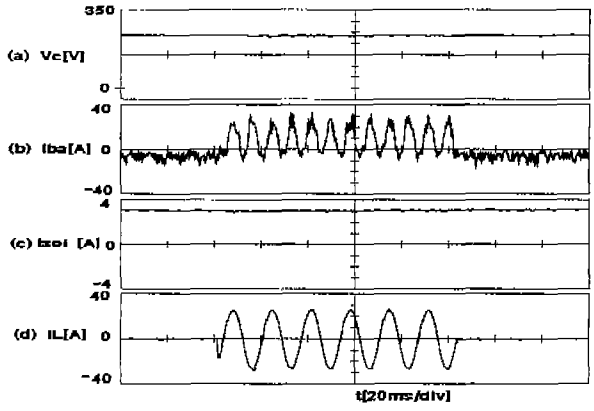

Fig. 16 Operating mode transition characteristics
(a) DC voltage (b) battery current
(c) solar cell current (d) load current

6. Conclusion

In this paper, controller of SPVS was designed and verified by experiment. System controller was based on 2 loop control contruction and feedforward control using power balance equation. In charge-discharge controller, feedforward control guarantee good transient response. But peak current increase made power component to be larger than when not using feedforward control. Therefore controller which have fast response and can suppress peak current increase should be researched. As futher study, in order to develope commonly used system , data acquisition and performance investigation based on field test should be done.

Rcferences

[1] M. G. Lee et al., " A Study on Optimization and Performance Analysis of PV System for Inhabited Remote Islands" KEPRI in Kora Technical ReportTM.95YT23.97.637

[2] H. Kobayashi, " Optimum Storage Battery Voltage for Photovoltaic System", CRIEPI in Japan Technical Report, T91071.

[3] H. Kobayashi, et al. " Storage Battery Operation Technique of Photovoltaic System" CRIEPI in Japan Technical Report T91071.

[4] LANDAU, " System Identification And Control Design", Prentice hall, 1990.

[5] K.J. Astrom, et al., "Automatic tuning of PID Controller", Instrument Society of America, 1988.

[6] Ned Mohan, et al.,"POWER ELECTRONICS: converters, applications and design", John Wiley & Sons, 1989.